Sensors and Actuators A 189 (2013) 161–167

Contents lists available at SciVerse ScienceDirect

Sensors and Actuators A: Physical

journal homepage: www.elsevier.com/locate/sna

Chaos based neural network optimization for concentration estimation of indoor air contaminants by an electronic nose

Lei Zhang[a,*], Fengchun Tian[a], Shouqiong Liu[b], Jielian Guo[a], Bo Hu[a], Qi Ye[a], Lijun Dang[a], Xiongwei Peng[a], Chaibou Kadri[a], Jingwei Feng[a]

[a] College of Communication Engineering, Chongqing University, 174 ShaZheng street, ShaPingBa District, Chongqing 400044, China
[b] Academy of Metrology and Quality Inspection, Chongqing 401123, China

ARTICLE INFO

Article history:
Received 1 July 2012
Received in revised form 5 October 2012
Accepted 18 October 2012
Available online xxx

Keywords:
Electronic nose
Artificial olfactory system
Back-propagation neural network
Chaotic sequence optimization
Particle swarm optimization

ABSTRACT

Electronic nose (E-nose), as an artificial olfactory system, can be used for estimation of gases concentration combined with a pattern recognition module. This paper studies the concentration estimations of indoor contaminants for air quality monitoring in dwellings using chaos based optimization artificial neural network integrated into our self-designed portable E-nose instrument. Back-propagation neural network (BPNN) has been recognized as the common pattern recognition. Considering the local optimal flaw of BPNN, this paper presents a novel chaotic sequence optimization BPNN method for improving the accuracy of E-nose prediction. Further comparison with particle swarm optimization is also employed, and maximum 26.03% and 16.4% prediction error decreased after using chaotic based optimization for formaldehyde and benzene concentration estimation. Experimental results demonstrate the superiority and efficiency of the portable E-nose instrument integrated with artificial neural network optimized by chaotic sequence based optimization algorithms in real-time monitoring of air quality in dwellings.

1. Introduction

An electronic nose can be a better alternative to conventional methods for continuous and real-time monitoring of air quality indoor in dwellings or in a car as a portable E-nose instrument. Four classes of contaminants (physical, chemical, biological and radioactive) were reported in indoor air quality standard [1]. Chemical contaminants including sulfur dioxide, nitrogen dioxide, carbon monoxide, carbon dioxide, ammonia, ozone, formaldehyde, benzene, toluene, inhalable particle, and volatile organic compounds were recognized as harmful substances to public health indoor [1]. The common contaminants in people's dwellings which we mainly aim to employ in our project using E-nose technology contain formaldehyde and benzene. These odorants have been mostly investigated for their potential harms to public health as pollutants of indoor air quality from numerous studies [1–3]. Besides, the emissions from new furniture, oil paint, and building materials of residuals often contain formaldehyde and benzene [4].

Chaos is a bounded unstable dynamic behavior that exhibits sensitive dependence on initial conditions and also unstable periodic motions in nonlinear systems [5]. Although it appears to be stochastic, it occurs in a deterministic nonlinear system under deterministic conditions. Chaotic sequences generated from many chaotic maps commonly possess certainty, ergodicity and stochastic property, and therefore they have been used instead of random sequences and somewhat good results have also been demonstrated when combined with particle swarm optimization [6] for global solutions search. In prediction, classification, and pattern recognition, hybrid forecasting models based on chaotic mapping have been presented together with Gaussian support vector machine, particle swarm optimization and genetic algorithm in [7,8]. Similarly, chaos optimization has also been used in prediction of silicon content in hot metal [9] and faults classification [10,11]. Chaos search immune algorithms have been presented in [12,13] for neuro-fuzzy controller design and pattern recognition. The choice of chaotic sequences is justified theoretically by their unpredictability including spread-spectrum characteristic, non-periodic, complex temporal behavior, and ergodic properties.

Electronic nose, as an artificial olfactory system, includes a central process unit, chemical gas sensor array, other peripheral circuits and pattern recognition module [14]. It has been widely used for analysis of volatile organic compounds [15], vapor chemicals [16], waters [17], wine [18] and breath alcohol measurement [19]. Neural network, especially back-propagation neural network (BPNN), has been widely used for recognition and function approximation based its strong regression ability [20]. So, in this paper, BPNN is used for concentration estimation of formaldehyde in an electronic nose. However, BP neural network still posses some

* Corresponding author. Tel.: +86 13629788369; fax: +86 23 65111745.
E-mail address: leizhang@cqu.edu.cn (L. Zhang).

0924-4247/$ – see front matter © 2012 Elsevier B.V. All rights reserved.
http://dx.doi.org/10.1016/j.sna.2012.10.023

inherent problems. First, BP model can easily get trapped in local minima for the problems of pattern recognition and complex functions approximation [21], so that a local optimal solution is obtained. Second, the solutions are different for every train with the random initial weights.

Particle swarm optimization (PSO) developed by Kennedy and Eberhart in 1995 [22] has been widely used in engineering application for best solution search and its superiority has attracted many researchers in forecasting [9–11]. However, in this paper, we present a novel mutative scale chaotic sequence method to optimize the weights of BPNN considering the characteristic of ergodicity. Two kinds of chaotic mapping equations with tent map and logistic map have been used for generation of chaotic sequences. Besides, PSO is also developed in neural network optimization for concentration estimation by an E-nose for comparisons.

2. Materials and methods

2.1. Our electronic nose

Our sensor array in E-nose system consists of four gas sensors from the TGS series including TGS2602, TGS2620 and TGS2201 with dual outputs (TGS2201A and TGS2201B). The characteristics of these sensors have been listed in Table 1 which demonstrates the detected gases and applications. Also, we refer readers to the sensors' datasheets for more information on TGS sensors available in http://www.figaro.co.jp/en/product/index.php?mode=search&kbn=1. In addition, a module (SHT2230 of Sensirion in Switzerland) with two auxiliary sensors for the temperature (T) and humidity (H) are also used for compensation. The sensors were mounted on a custom designed printed circuit board (PCB), along with associated electrical components. A 12-bit analog-digital (A/D) converter with type of TLC2543 is used as interface between the Field Programmable Gate Array (FPGA) processor represented as the central processor unit (CPU) and the sensors. A Synchronous Dynamic Access Memory (SDRAM) connected with FPGA processor is used for data collection, storage and processing. The E-nose system designed with FPGA processor and other peripheral circuits is connected to a personal computer (PC) via a Joint Test Action Group (JTAG) port which can be used to transfer data and debug programs. An input vector with 6 variables can be obtained in each observation; the multidimensional response data set presents a nonlinear relation with the target gas concentration. Formaldehyde and benzene measurements were employed by an E-nose in the constant temperature and humidity chamber in which the temperature and humidity can be effectively controlled in terms of the target temperatures and humidity. Note that the precisions of the chamber for temperature and humidity are $\pm 0.1\,^{\circ}C$ and $\pm 5\%$RH. The self-designed electronic nose is shown in Fig. 1. The left picture in Fig. 1 denotes the impression of the product, and the right one in Fig. 1 denotes the internal PCB with integrated circuits including the main modules highlighted.

2.2. Data acquisition

In terms of the indoor monitoring of the formaldehyde and benzene concentrations, formaldehyde and benzene were measured at the concentration range of 0–10 ppm, respectively, target temperatures of 15, 25, 30 and 35 °C and target humidity of 40%, 60%, 80%RH (relative humidity) in order to imitate the real environment indoor. For each measurement, the total measurement cycle time for one single measurement was set to 20 min, i.e. 2 min for reference air (baseline), 8 min for gas sampling and 10 min for cleaning of the chamber through injecting clean air before the next measurement begins. Totally, 116 observation samples were collected. For model building of formaldehyde monitoring, 71 training samples, 25 test samples and 20 validation samples were divided from the whole sample set. Also, for model building of benzene monitoring, 40 training samples, 22 test samples and 10 validation samples were divided from the whole sample set. The actual concentration of formaldehyde for each sample was obtained through the spectrophotometer analysis of the chemical sampling using the air sampler. The actual concentration of benzene is analyzed using gas chromatograph (GC). In detail, Table 2 presents the specific experimental samples of formaldehyde and benzene with different combinations of temperature (T) and relative humidity (RH). 12 combinations {(15, 60), (15, 80), (20, 40), (20, 80), (25, 40), (25, 60), (25, 80), (30, 40), (30, 60), (30, 80), (35, 40), (35, 60)} in manner of (T, RH) were employed for covering the indoor conditions. From Table 2, we can find that various concentrations were employed for estimation model construction considering the various environments in dwellings. For each sample, a vector with 6 variables was extracted at the steady state response. Besides, a simple normalization method divided by 4095 was used for subsequent pattern analysis in voltage. Notice that 4095 is calculated as $2^{12}-1$ with the principle of 12-bit A/D converter. The specific experimental platform is illustrated in Fig. 2 which has been used in our previous publication [23]. Five ports (ports_1–5) are used in the chamber. Port_1 is used for injection of contaminants, port_2 is used to clean the chamber through injection of fresh air, port_3 is set to control the relative humidity in the chamber by using a humidifier with a valve, port_4 is for data collection by connecting the electronic nose instrument to the PC with a JTAG and port_5 is set to sampling by a gas sampler for sample's concentration analysis using spectrophotometer and GC.

2.3. Back-propagation neural network

Back-propagation algorithm (BP) with a gradient descending strategy was proposed in [24]. Rumelhart further formulated the standard back propagation algorithm (BP) for multilayered perceptrons. The architecture of a multilayered perceptron neural network is shown in Fig. 3 which presents a two hidden layered BP neural network. BP neural network has been widely used to classify nonlinearly separable patterns in real application for its strong ability in recognition [25]. However, BP neural network still posses some inherent problems. First, BP model can easily get trapped in local minima for the problems of pattern recognition, and fail to find the global optimal solution. Second, the initial weight matrix **W** and bias vectors **B** of back-propagation neural network are randomly produced for training so that different weights and biases would produce different trained neural networks. Thus, obtaining the global minimum of regression error by only using back propagation neural network becomes little impractical. In our previous work, we have employed these problems using heuristic and bio-inspired methods [20].

2.4. Mutative scale chaotic sequence optimization

Chaos optimization is developed using chaotic variables. Three chaos map equations were studied in this paper. The logistic map is shown by

$$z_k = \mu \cdot z_k \cdot (1 - z_k) \tag{1}$$

where z_k is the k-th chaotic variable and k denotes the iteration number. Obviously, $z_k \in (0,1)$ under the conditions that the initial $z_0 \in (0,1)$ and the z_0 cannot be the digits of {0, 0.25, 0.75, 1}. Here, $\mu = 4$ can be a completely chaotic state.

Table 1
Characteristics of the sensors in use.

Sensor type	Objectives	Applications
TGS2602	High sensitivity to VOCs, odorous gases, gaseous air contaminants;	Air cleaners, ventilation control, air quality, VOC, and odor monitors;
TGS2620	High sensitivity to alcohol and organic solvent vapors;	Alcohol testers, organic vapor detectors/alarms, solvent detectors;
TGS2201A	Sensitivity to diesel exhaust gas NO_x;	Automobile ventilation control, air contaminants detection;
TGS2201B	Sensitivity to gasoline exhaust gas CO, H_2, etc.	Automobile ventilation control, air contaminants detection.

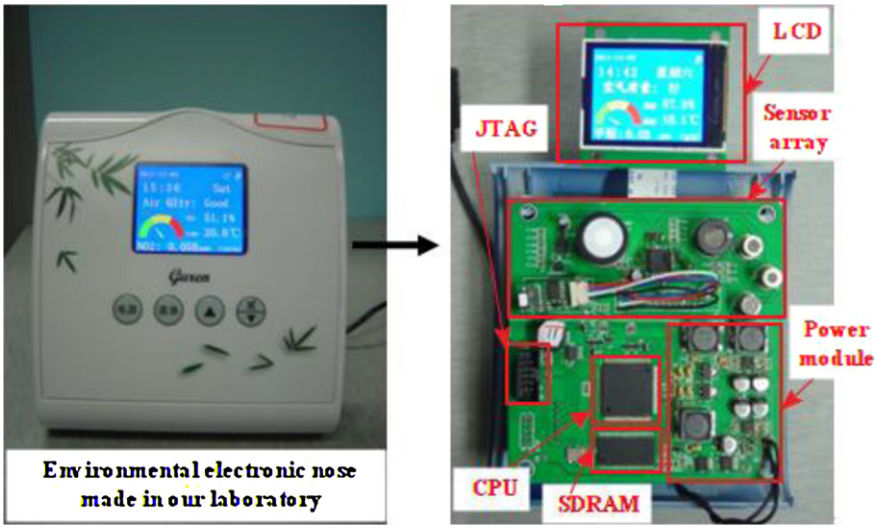

Fig. 1. Self-designed electronic nose for indoor air quality monitoring. The left picture is the integral electronic nose; the right picture is the internal PCB with integrated circuits with the main modules labeled.

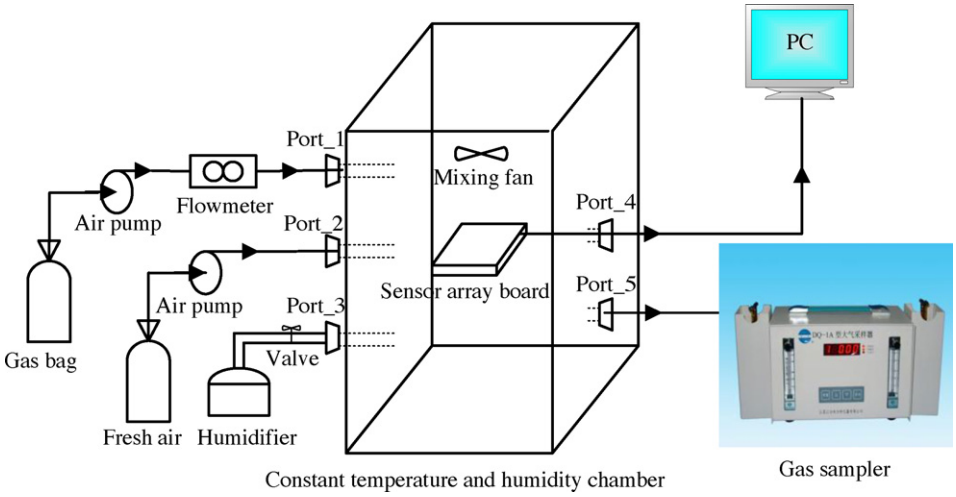

Fig. 2. Schematic of the experimental platform with our designed electronic nose system.

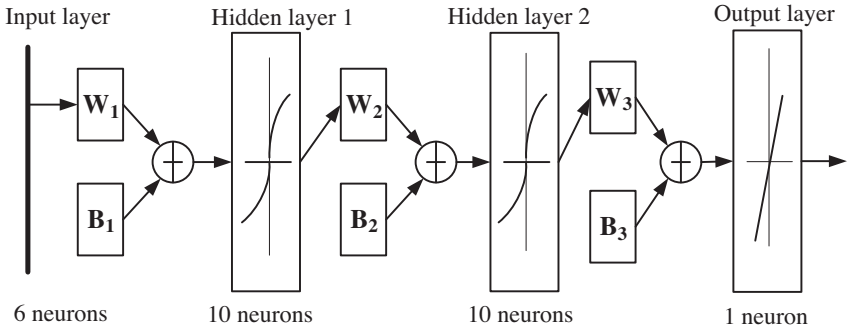

Fig. 3. Architecture of neural network with two hidden layers.

Table 2
Concentration (ppm) conditions of all experimental samples in different combinations (*T*, RH) in which *T* denotes temperature and RH (%) denotes relative humidity.

(15, 60)	(15, 80)	(20, 40)	(20, 60)	(20, 80)	(25, 40)	(25, 60)	(25, 80)	(30, 40)	(30, 60)	(30, 80)	(35, 40)	(35, 60)
Conditions of formaldehyde samples												
0.22	0.10	0.07	0.08	0.08	0.13	0.05	0.04	0.10	0.13	0.09	0.08	0.04
0.25	0.16	0.14	0.10	0.06	0.07	0.10	0.04	0.23	0.06	0.20	0.21	0.12
0.19	0.14	0.16	0.24	0.11	0.14	0.08	0.20	2.61	0.16	0.25	0.12	0.09
0.20	1.44	0.07	0.10	0.24	0.26	0.11	0.25	1.42	0.22	0.10	0.21	0.04
0.06	0.56	0.09	0.18	0.13	0.21	0.17	0.07		0.15	0.13	2.46	0.17
0.08		2.62	4.53	0.15	0.17	0.26	0.25		3.67	2.22	2.28	0.25
0.12		1.05	1.09	3.17	0.22	0.24	0.11		2.40	1.78		0.04
0.71				0.47	1.73	0.17	2.13					0.17
0.77					1.23	0.27	1.76					1.04
1.06						0.22						1.42
2.68						0.25						5.32
0.92						0.11						1.36
1.87						0.23						3.51
						0.25						
						0.12						
						1.22						
						2.38						
						1.75						
						3.00						
						1.28						
						2.99						
Conditions of benzene samples												
0.17	0.17	0.17	0.17	0.17	0.17	0.17	0.17	0.17	0.17	0.17	0.17	0.17
0.28	0.28	0.28	0.28	0.28	0.28	0.28	0.28	0.28	0.28	0.28	0.28	0.28
0.49	0.49	0.49	0.49	0.49	0.49	0.49	0.49	0.49	0.49	0.49	0.49	0.49
0.91	0.91	0.91	0.91	0.91	0.91	0.91	0.91	0.91	0.91	0.91	0.91	0.91
0.71	0.71	0.71	0.71	0.71	0.71	0.71	0.71	0.71	0.71	0.71		0.71
0.11	0.06	0.09	0.08	0.20	0.19	0.15	0.15					

The tent map [6] resembles the logistic map. It can also generate chaotic queue in (0, 1) in terms of the following form

$$z_k = \begin{cases} z_k/0.7 \quad , z_k < 0.7 \\ 10/3 \cdot z_k \cdot (1 - z_k), z_k \geq 0.7 \end{cases} \tag{2}$$

The Gauss map [6] which can also generate a chaotic queue in (0, 1) can be represented by

$$z_{k+1} = \begin{cases} 0, z_k = 0 \\ 1/z_k - \left\lfloor 1/z_k \right\rfloor , z_k \in (0, 1) \end{cases} \tag{3}$$

where $\lfloor x \rfloor$ denotes the largest integer less than x.

The algorithm procedure of mutative scale chaotic sequence optimization neural network can be concluded as follows

Step 1: Initialization $g = 0$. Randomly generates one M-dimensional population $\mathbf{X}^0$ with N individuals within (0, 1) and determine the initial optimization boundary $[\boldsymbol{a}, \boldsymbol{b}]$ in the optimization space.

Step 2: Map the variable $\mathbf{X}_i^k$ into the optimization space and obtain one new population $\mathbf{MX}_i^k$ using the following equation

$$MX_i^k = a_i^k + MX_i^k(b_i^k - a_i^k), i = 1, \ldots, N; k = 1, \ldots, M \tag{4}$$

Step 3: Evaluate the new population **MX** using BPNN algorithm and find the best individual **Xgbest**. The cost function has been defined as the maximum absolute relative error of the train and test samples shown by

$$f = \max \left\{ 1/n_1 \cdot \sum_{i=1}^{n_1} |ytr_i - ttr_i|/ttr_i, 1/n_2 \cdot \sum_{j=1}^{n_2} |yte_j - tte_j|/tte_j \right\} \times 100 \tag{5}$$

where n_1 and n_2 denote the number of train samples and test samples; **ytr** and **ttr** denote the predictive concentrations and actual concentrations of train samples; **yte** and **tte** denote the predictive concentrations and actual concentrations of test samples. Note that a decoding of **MX** for the initial weights and bias of the neural network is necessary, because each individual is encoded as the weights and bias.

Step 4: Mutative scale of chaotic variable search.

If the best solution keeps invariant within T iterations, the shrink of the search boundary $[a, b]$ can be performed using the following strategy for specific search in a smaller space

$$\mathbf{a}^{g+1} = \mathbf{Xgbest} - \gamma^g \cdot (\mathbf{b}^g - \mathbf{a}^g) \tag{6}$$

$$\mathbf{b}^{g+1} = \mathbf{Xgbest} + \gamma^g \cdot (\mathbf{b}^g - \mathbf{a}^g) \tag{7}$$

$$\gamma^{g+1} = \beta_1 \cdot \gamma^g \tag{8}$$

where $\mathbf{a}^{g+1}$ and $\mathbf{b}^{g+1}$ denote the new search boundary, γ is the radius of search, β_1 denotes decay coefficient less than 1.

Step 5: The constraints process of the boundary using the following strategy

$$\text{If} \quad a_i^k < -C^g, \quad a_i^k = -C^g; \quad \text{if} \quad b_i^k > C^g, \quad b_i^k = C^g \tag{9}$$

$$C^{g+1} = \beta_2 \cdot C^g \tag{10}$$

where C denotes the maximum boundary and β_2 denotes the attenuation coefficient similar to simulated annealing.

Step 6: if the current solution satisfies the termination criteria or that the maximization iterations finished, stop; else go to step 7.

Step 7: Generate the new population X using the chaotic map equations, and go to step 2.

2.5. Standard particle swarm optimization (SPSO)

In this standard PSO system, a number of particles cooperate to search for the best solutions by simulating the movement and flocking of birds [22]. These particles fly with a certain velocity and find the global best position after certain generations. At each generation t, the velocity is updated and the particle is moved to a new position. This new position is simply calculated as the sum of the previous position and the new velocity. The mathematical description of PSO is defined as follows

Suppose the dimension for a searching space is D, the total number of particles is N, the position of the i-th particle can be expressed as vector $\mathbf{X}_i = (x_{i1}, x_{i2}, \ldots, x_{iD})$; the best position of the i-th particle searching until now is $\mathbf{P}_i = (p_{i1}, p_{i2}, \ldots, p_{iD})$; the best position of all the particles searching until now is $\mathbf{P}_g = (p_{g1}, p_{g2}, \ldots, p_{gD})$; the velocity of the i-th particle is represented as $\mathbf{V}_i = (v_{i1}, v_{i2}, \ldots, v_{iD})$, then the standard PSO can be illustrated as

$$v_{id}(t+1) = w \cdot v_{id}(t) + c_1 \cdot r_{1i}^p(t) \cdot [p_{id}(t) - x_{id}(t)] + c_2 \cdot r_{2i}^p(t) \cdot [p_{gd}(t) - x_{id}(t)] \quad (11)$$

$$x_{id}(t+1) = x_{id}(t) + v_{id}(t+1); 1 \le i \le N, 1 \le d \le D \quad (12)$$

where c_1, c_2 are the acceleration constants with positive values; w is called inertia factor;

$$r_{1i}^p(t) \leftarrow U(0,1), \quad r_{2i}^p(t) \leftarrow U(0,1) \quad (13)$$

Noteworthy is that, placing a limit on the velocity $v_{\max}$ and adjusting the inertia weight w, the PSO can achieve better search performance.

$$v_p^i(t+1) = \begin{cases} v_{\max}^i, v_p^i(t+1) > v_{\max}^i \\ -v_{\max}^i, v_p^i(t+1) < -v_{\max}^i \\ v_p^i(k+1), \text{otherwise} \end{cases} \quad (14)$$

In this paper, the inertia weights w is updated through a cosine mechanism by

$$w(t) = w_{start} + w_{end} \cdot \cos(t/10) \quad (15)$$

where w_{start} is the initial value, and w_{end} is the terminal value. In this work, w_{start} and w_{end} are set as 0.85 and 0.45, respectively.

2.6. Parameter settings

Due to that the determination of the number of hidden layers and neurons in neural network cannot be fixed theoretically, in this paper, a two hidden layered neural network whose structure is 6-10-10-1 was used for each gas monitoring in experience. Generally, the log-sigmoid function and pure linear function were used in the hidden layers and output layer, respectively. In terms of the network structure, matrix $\mathbf{W}_1$ (10×6), $\mathbf{W}_2$ (10×10) and $\mathbf{W}_3$ (1×10) represent the weights between the input layer and the hidden layer-1, the hidden layer-1 and the hidden layer-2, the hidden layer-2 and the output layer; vectors $\mathbf{B}_1$ (10×1), $\mathbf{B}_2$ (10×1) and $\mathbf{B}_3$ (1×1) represent the bias in hidden layer-1, hidden layer-2 and output layer. An individual $\mathbf{L} = [l_1, l_2, \ldots, l_N]$ can be shown as follow

$$\overbrace{l_1, \ldots, l_{60}}^{\mathbf{W}_1}, \overbrace{l_{61}, \ldots, l_{70}}^{\mathbf{B}_1}, \overbrace{l_{71}, \ldots, l_{170}}^{\mathbf{W}_2}, \overbrace{l_{171}, \ldots, l_{180}}^{\mathbf{B}_2}, \overbrace{l_{181}, \ldots, l_{190}}^{\mathbf{W}_3}, \overbrace{l_{191}}^{\mathbf{B}_3} \quad (16)$$

Therefore, the length N of one individual $\mathbf{L}$ can be calculated as $N = 6 \times 10 + 10 + 10 \times 10 + 10 + 10 \times 1 + 1 = 191$.

The training goal of neural network is dynamically set as 0.05–0.5 for formaldehyde, and 0.005–0.05 for benzene. Consider the long running time of the whole algorithm, the size M of population is set as 50, the maximum iterations $G_1 = 100$ for formaldehyde, and $G_2 = 10$ for benzene, and the permissible iterations $T = 10$ for stagnation. The initial boundaries of $\mathbf{a}$ and $\mathbf{b}$ are set as -20 and 20, and $C = 20$. Besides, the decay coefficient β_1 and attenuation coefficient β_2 are set as 0.98 and 0.95, respectively. The initial search radius γ is set as 0.2. The fitness function f in each optimization is set as the maximum relative error of the average relative training error and the average relative test error shown as Eq. (5). It is worthy noting that the parameters settings are experienced and can be adjusted according to respective optimization problem.

2.7. On-line use

The whole chaos and PSO based neural network optimization and learning algorithms are implemented in PC for learning the best weights $\mathbf{W} = \{\mathbf{W}_1, \mathbf{W}_2, \mathbf{W}_3\}$ and $\mathbf{B} = \{\mathbf{B}_1, \mathbf{B}_2, \mathbf{B}_3\}$ of the neural network, and then $\mathbf{W}$ and $\mathbf{B}$ would be transferred to the E-nose system for prediction on line. In real-time application of the E-nose instrument, the forward computation process of neural network without backpropagation will be implemented in FPGA combined with learned neural network weights $\mathbf{W}$ and $\mathbf{B}$ for concentration estimation. The forward computation process in FPGA is illustrated as three steps:

Step 1: $\mathbf{y}_1 = 1/[1 + e^{-(\mathbf{W}_1 \cdot \mathbf{x} + \mathbf{B}_1)}]$
Step 2: $\mathbf{y}_2 = 1/[1 + e^{-(\mathbf{W}_2 \cdot \mathbf{y}_1 + \mathbf{B}_2)}]$
Step3: $\mathbf{y}_3 = \mathbf{W}_3 \cdot \mathbf{y}_2 + \mathbf{B}_3$

where $\mathbf{x}$ is the real-time observation vector of the sensor array, $\mathbf{y}_1$ is the output vector of the first hidden layer with a log-sigmoid transfer function, $\mathbf{y}_2$ is the output vector of the second hidden layer with a log-sigmoid transfer function and $\mathbf{y}_3$ is the final output of the neural network prediction with a pure linear function.

3. Results and discussion

The estimation results for the formaldehyde and benzene experiments analyzed using the chaotic sequence optimization neural network and standard particle swarm optimization (PSO) neural network have been presented in this section. The model building is based on the train samples and test samples. The role of the test samples is used to control the possible overfitting of training samples and evaluate the fitness function of chaotic sequence and PSO optimization. We apply the maximum relative error of training and test samples as the fitness function to improve the robustness of the model. The validation samples are finally used to verify the efficiency of the model. Fig. 4 illustrates the formaldehyde prediction results of the test samples (left) and validation samples (right) using four optimization methods combined with BPNN. Similarly, Fig. 5 illustrates the benzene predictions of the test samples (left) and validation samples (right) using four optimization BPNN methods. From the trace of predictions and actual concentrations, we can find that the four methods can track the actual concentrations approximately. The predicted curve using chaos with logistic map can approach the actual curve better for formaldehyde concentration estimation. However, for benzene estimation, chaos method with Gaussian map presents a better prediction. For quantification of the prediction error, Table 3 presents the relative prediction error using four optimization methods. From this table, we can find that the chaotic sequence optimization with logistic map has the minimum prediction error 32.34% of formaldehyde validation samples and 26.03% error decreased compared with the prediction error 58.37% using single neural network. And Gaussian map obtains the minimum prediction error 13.31% of benzene validation samples and 16.4% error decreased compared with the predictor error 29.71% using single neural network. Due to that the neural network is trained separately for each gas, therefore in real time application of our electronic nose for formaldehyde and benzene estimation, the best neural network with minimum prediction error is selected for each gas monitoring.

From the analysis of estimation results, the optimization methods are effective for neural network optimization. From the comparisons of chaotic sequence methods and PSO on the results, we cannot definitely decide which one has better optimization ability because their prediction difference for each gas is not very obvious. However, from the characteristic of chaotic sequence, the

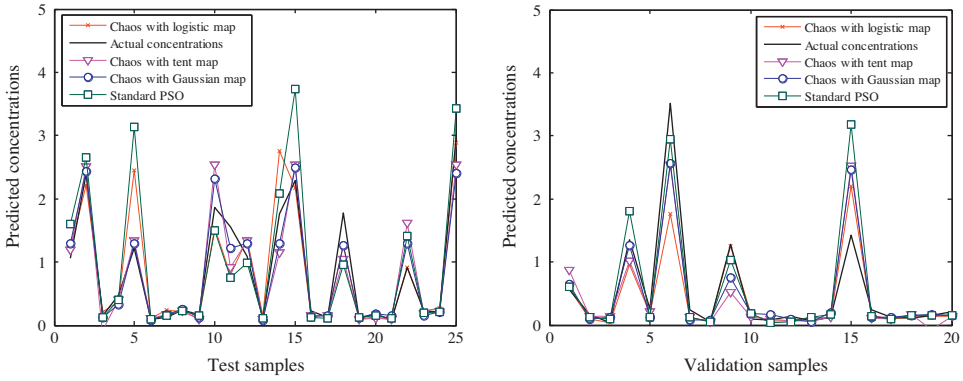

Fig. 4. Formaldehyde prediction results of the test samples (left) and validation samples (right) using four optimization methods.

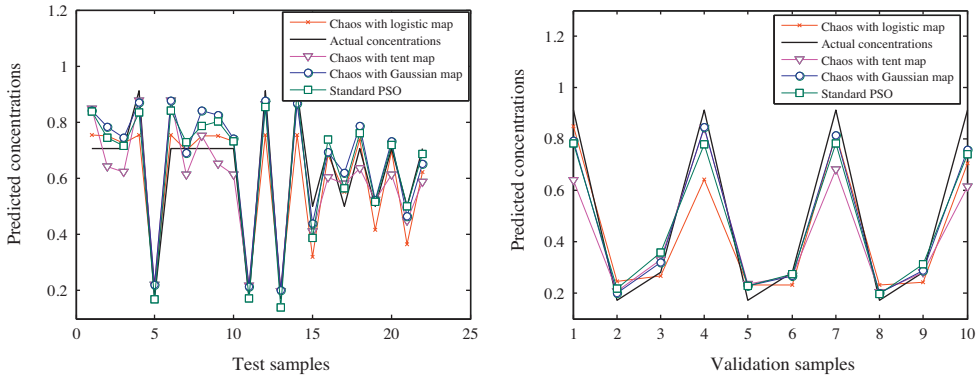

Fig. 5. Benzene prediction results of the test samples (left) and validation samples (right) using four optimization methods.

Table 3
Relative prediction error using different optimization neural network methods.

Estimation models	Relative prediction error (%)					
	Formaldehyde			Benzene		
	Train	Test	Validation	Train	Test	Validation
Single BP	46.55	40.38	58.37	27.18	16.53	29.71
Logistic map-BP	28.35	28.89	32.34	16.57	12.15	17.96
Tent map-BP	29.78	30.27	49.49	8.910	13.12	19.16
Gaussian map-BP	30.06	23.06	50.64	11.62	11.73	13.31
Standard PSO-BP	29.94	29.56	47.06	12.49	12.21	16.08

ergodicity of chaos can help to find the global optimal in optimization after a number of generations. However, PSO has a fast convergence performance and get to a local optimal in a short time. So, researchers can decide which optimization can be used in terms of their need.

4. Conclusions

This paper presents a novel chaos sequence optimization neural network method for concentration prediction of formaldehyde and benzene in dwellings by a portable electronic nose. For comparison, PSO is also used for optimization. Through the formaldehyde and benzene samples obtained in experiments combined with the self-designed electronic nose, we built the neural network prediction model combined with the chaos optimization and PSO, respectively. By comparison of the prediction error of models based on chaotic sequence and PSO, both methods are effective for weights optimization. The neural network has been improved to a large extent and the concentration estimations for formaldehyde and benzene indoor have also been realized in our project.

Acknowledgements

We would like to express our sincere appreciation to the anonymous reviewers for their insightful comments, which have greatly improved the quality of the paper.

This work was supported by the Key Science and Technology Research Program (No. CSTC2010AB2002, CSTC2009BA2021) and Chongqing University Postgraduates' Science and Innovation Fund (No. CDJXS12160005). This work was also funded by New Academic Researcher Award for Doctoral Candidates granted by Ministry of Education in China.

References

[1] A.P. Jones, Indoor air quality and health, Atmospheric Environment 33 (1999) 4535–4564.
[2] S.C. Lee, M. Chang, Indoor and outdoor air quality investigation at schools in Hong Kong, Chemosphere 41 (2000) 109–113.
[3] S. De Vito, E. Massera, M. Piga, L. Martinotto, G. Di Francia, On field calibration of an electronic nose for benzene estimation in an urban pollution monitoring scenario, Sensors and Actuators B 129 (2008) 750–757.

[4] H. Huang, F. Haghighat, Modelling of volatile organic compounds emission from dry building materials, Building and Environment 37 (2002) 1349–1360.
[5] H.G. Schuster, Deterministic Chaos: An Introduction, Physick-Verlag GmnH, Weinheim, Federal Republic of Germany, 1988.
[6] B. Alatas, E. Akin, A. Bedri Ozer, Chaos embedded particle swarm optimization algorithms, Chaos, Solitons and Fractals 40 (2009) 1715–1734.
[7] Q. Wu, A hybrid-forecasting model based on Gaussian support vector machine and chaotic particle swarm optimization, Expert Systems with Applications 37 (2010) 2388–2394.
[8] Q. Wu, The hybrid forecasting model based on chaotic mapping, genetic algorithm and support vector machine, Expert Systems with Applications 37 (2010) 1776–1783.
[9] X. Tang, L. Zhuang, C. Jiang, Prediction of silicon content in hot metal using support vector regression based on chaos particle swarm optimization, Expert Systems with Applications 36 (2009) 11853–11857.
[10] C. Zhao, X. Sun, S. Sun, J. Ting, Fault diagnosis of sensor by chaos particle swarm optimization algorithm and support vector machine, Expert Systems with Applications 38 (2011) 9908–9912.
[11] X. Tang, L. Zhuang, J. Cai, C. Li, Multi-fault classification based on support vector machine trained by chaos particle swarm optimization, Knowledge-Based Systems 23 (2010) 486–490.
[12] X.Q. Zuo, Y.S. Fan, A chaos search immune algorithm with its application to neuro-fuzzy controller design, Chaos, Solitons and Fractals 30 (2006) 94–109.
[13] Z. Guo, S. Wang, J. Zhuang, A novel immune evolutionary algorithm incorporating chaos optimization, Pattern Recognition Letters 27 (2006) 2–8.
[14] M.S. Simon, D. James, Z. Ali, Data analysis for electronic nose systems, Microchimica Acta 156 (2007) 183–207.
[15] J.E. Haugen, K. Kvaal, Electronic nose and artificial neural network, Meat Science 49 (1998) S273–S286.
[16] L. Carmel, N. Sever, D. Lancet, D. Harel, An eNose algorithm for identifying chemicals and determining their concentration, Sensors and Actuators B 93 (2003) 77–83.
[17] E.G. Breijo, J. Atkinson, L.S. Sanchez, A comparison study of pattern recognition algorithms implemented on a microcontroller for use in a electronic tongue for monitoring drinking waters, Sensors and Actuators A 172 (2011) 570–582.
[18] L.G. Sanchez, J. Soto, M.R. Martinez, A novel humid electronic nose combined with an electronic tongue for assessing deterioration of wine, Sensors and Actuators A 171 (2011) 152–158.
[19] N. Paulsson, E. Larsson, F. Winquist, Extraction and selection of parameters for evaluation of breath alcohol measurement with an electronic nose, Sensors and Actuators A 84 (2000) 187–197.
[20] L. Zhang, F. Tian, C. Kadri, G. Pei, H. Li, L. Pan, Gases concentration estimation using heuristics and bio-inspired optimization models for experimental chemical electronic nose, Sensors and Actuators B 160 (2011) 760–770.
[21] M. Gori, A. Tesi, On the problem of local minima in back-propagation, IEEE Transactions on Pattern Analysis and Machine Intelligence 14 (1) (1992) 76–86.
[22] J. Kennedy, R.C. Eberhart, Particle swarm optimization, Proceedings of IEEE International Conference on Neural Networks 4 (1995) 1942–1948.
[23] L. Zhang, F. Tian, H. Nie, L. Dang, G. Li, Q. Ye, C. Kadri, Classification of multiple indoor air contaminants by an electronic nose and a hybrid support vector machine, Sensors and Actuators B 174 (2012) 114–125.
[24] W. Wu, J. Wang, M.S. Cheng, Z.X. Li, Convergence analysis of online gradient method for BP neural networks, Neural Networks 24 (2011) 91–98.
[25] J.R. Zhang, J. Zhang, A hybrid particle swarm optimization back-propagation algorithm for feed-forward neural network training, Applied Mathematics and Computation 185 (2007) 1026–1037.

Biographies

Lei Zhang received his bachelor degree in electrical/electronics engineering in 2009 from the Nanyang Institute of Technology, China; from September 2009 to December 2010, he studied for a MS degree in signal and information processing. He is presently with Chongqing University, pursuing his PhD degree in circuits and systems. His research interests include computational intelligence, artificial olfactory system, and nonlinear signal processing in electronic nose.

Fengchun Tian received PhD degree in 1997 in electrical engineering from Chongqing University. He is currently a professor with the College of Communication Engineering of Chongqing University. His research interests include electronic nose technology, artificial olfactory systems, pattern recognition, chemical sensors, signal/image processing, wavelet, and computational intelligence. In 2006 and 2007, he was recognized as a part-time professor of GUELPH University, Canada.

Shouqiong Liu is now a senior engineer of Academy of Metrology And Quality Inspection, Chongqing. Her research interest was mainly analytical chemistry.

Jielian Guo received her bachelor degree in communication engineering in 2010 from the Chongqing University, China; from September 2010 to June 2012, she studied for a MS degree in circuits and system. Her research interests include circuits and system design in electronic nose technology.

Bo Hu received his bachelor degree in communication engineering in 2010 from the Chongqing University, China; from September 2010 to June 2012, he studied for a MS degree in circuits and system. His research interests include circuits and system design in electronic nose technology.

Qi Ye received his bachelor degree in communication engineering in 2010 from the Chongqing University, China; from September 2010 to June 2012, he studied for a MS degree in circuits and system. His research interests include circuits and system design in electronic nose technology.

Lijun Dang received her bachelor degree in school of electronic and information engineering in 2011 from the Dalian University of Technology, China; from September 2011 to June 2012, she studied for a MS degree in circuits and system. Her research interests include circuits and system design in electronic nose technology.

Xiongwei Peng received his bachelor degree in communication engineering in 2012 from the Chongqing University, China; from September 2012 to June 2014, he studied for a MS degree in circuits and system. His research interests include artificial neural network, genetic algorithms and optimizations.

Chaibou Kadri received his bachelor degree in electrical/electronics engineering in 2001 from the Federal University of Technology Bauchi, Nigeria; his MS degree in communication and information system in 2009, from Chongqing University China. He is presently with Chongqing University, pursuing his PhD degree in Circuits and Systems. His research interests include signal processing for gas sensors array instruments, and machine learning.

Jingwei Feng received his bachelor degree in communication from Chongqing University of China in 2009. He is currently pursuing the direct PhD degree in the same university. His research interests include signal processing patter recognition techniques applied to machine olfaction. He is currently working in the wound infection detection by electronic nose.